

# Torque Control of Brushless Direct Current Motor Drives using a Single Current Sensor with High Reliability

Mohsen Ebadpour<sup>1</sup>, AhadFarzinfar<sup>2</sup>

<sup>1,2</sup>Department of Electrical Engineering, Ahar Branch, Islamic Azad University, Ahar, Iran

Email: m.ebadpour@yahoo.com , ahad\_farzinfar@yahoo.com

## Abstract

*Due to the simple structure, high torque density, low maintenance, and high efficiency, brushless direct current (BLDC) motors are widely used in automation and industrial applications. A control strategy based on single current sensor is proposed for a four-switch three-phase BLDC motor system to lower cost and improve reliability. The whole working process of the BLDC motor is divided into six modes. Phase c involves four modes, including modes 2, 3, 5, and 6. Only one switch will work in these modes. In modes 1 and 4, two switches will work simultaneously and the current flows through phases a and b. Compared to the most recent and highly performed torque control strategy, the proposed strategy offers an improved reliability thanks to the achievement of balanced switching frequencies of the inverter upper and lower switches. Furthermore, the torque ripple is damped significantly during sector-to-sector commutations using a hysteresis current controller. The effectiveness of the proposed system has been validated by simulation results using MATLAB/Simulink software in various operation conditions.*

**Keywords:** Brushless Direct Current (BLDC) motor, Torque control, Current sensor four-switch inverter, High reliable control.

## 1- Introduction

In recent years, variable speed drives equipped with electrical motors are extensively integrated in various applications. Permanent magnet brushless direct current (BLDC) motors offer many advantages including high efficiency, low maintenance, greater longevity, reduced weight and more compact constructions. The BLDC motors have been widely used in a variety of applications in industrial automation and consumer appliances because of their high power density and ease of control [1], [2]. Nowadays, many studies have focused on how

to reduce the cost of the BLDC motor and its control system without performance degradation [3-5]. The cost reduction of variable-speed drives such as BLDC motor drives is accomplished by using two approaches. One is the topological approach and the other is the control approach. From a topology point of view, minimum number of switches and eliminating the mechanical sensors are required for the inverter circuit. In the control approach, algorithms are designed and implemented in conjunction with a reduced component inverter to produce the desired speed-torque characteristics [6].

In recent years, many researches have been conducted on cost-effective drives and control techniques for BLDC motors. In [7], a new speed control method using the acceleration feed-forward compensation is proposed to improve the speed response characteristic for a four-switch three-phase BLDC motor. The disturbance torque estimation method is adopted to improve the robustness of the method. An original study on the generated torque ripples due to phase commutation in the four-switch three-phase BLDC motor is presented in [8]. A current control technique is developed to minimize commutation torque for the entire speed range. An adaptive Neuro-fuzzy inference system controller is proposed in [9]. This developed design does not require an accurate model of the motor and has a fairly simple structure.

The four-space-vector scheme was used in [10], the six commutation modes based on current control by two current sensors. Some work has also been done on asensorless BLDC motor drives [11], [12].

In this paper, a cost-effective control strategy for four-switch three-phase BLDC motor drives using only a single current sensor is proposed. The proposed control strategy is based on only one hysteresis current controller for three phases. Moreover, a further attenuation of the torque ripple during commutation intervals has been gained thanks to the use of an appropriate torque controller. Section 2 explains the BLDC motor operation principle. In section 3, analysis of the proposed four-switch three-phase BLDC motor drive system based on single current control strategy is explained. Finally, simulation results are given section 4.

## 2- BLDC Motor Opration Pincipal

The BLDC motor employs a DC power supply switched to the stator phase windings of the motor by power devices, the switching sequence being determined from the rotor position. The phase current of BLDC motor, in typically rectangular shape, is synchronized with the back EMF to produce constant torque at a constant speed. Fig.1 shows the structure of a six-switch three-phase BLDC motor drive. These motors are driven by a three-phase inverter with a six-steps commutation. The conducting interval for each phase is  $120^\circ$  electrical degree. Therefore, only two phases conduct current at any time, leaving the third phase floating. The typical mathematical model of the BLDC motor is described as follows:

$$\begin{bmatrix} v_{aN} \\ v_{bN} \\ v_{cN} \end{bmatrix} = \begin{bmatrix} R & 0 & 0 \\ 0 & R & 0 \\ 0 & 0 & R \end{bmatrix} \begin{bmatrix} i_a \\ i_b \\ i_c \end{bmatrix} + \begin{bmatrix} L & 0 & 0 \\ 0 & L & 0 \\ 0 & 0 & L \end{bmatrix} \frac{d}{dt} \begin{bmatrix} i_a \\ i_b \\ i_c \end{bmatrix} + \begin{bmatrix} e_a \\ e_b \\ e_c \end{bmatrix} \quad (1)$$

$$L = (L_S - L_M) \quad (2)$$

Where,  $v_{aN}$  represents the terminal phase  $a$  voltage with respect to the star point,  $i_a$  is the rectangular-shaped phase  $a$  current,  $e_a$  is the trapezoidal-shaped back EMF, and  $R$ ,  $L_S$  and  $L_M$  are the resistance, self-inductance and mutual-inductance, respectively.

The electromagnetic torque is expressed as:

$$T_e = \frac{1}{\omega_r} (e_a i_a + e_b i_b + e_c i_c) \quad (3)$$

Where,  $\omega_r$  is the mechanical speed of the rotor and  $T_e$  is the electromagnetic torque. The equation of motion is:

$$\frac{d}{dt} \omega_r = (T_e - T_L - B\omega_r) / J \quad (4)$$

Where,  $B$  is the damping constant,  $J$  is the moment of inertia of the drive and  $T_L$  is the load torque.

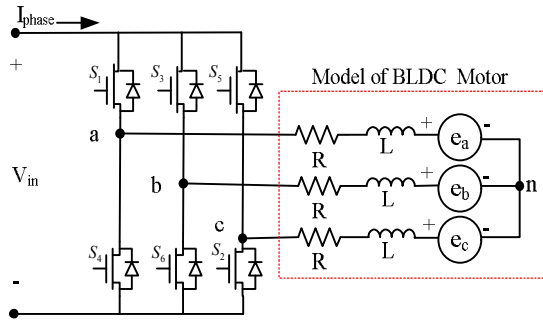


**Fig.1.** The structure of BLDC motor drive

The commutation timing is determined by the rotor position, which can be detected by Hall sensors or estimated from motor parameters if it is a sensorless system. For the three phases BLDC motor, the phase to phase back EMFs and phase current waveforms are shown in Fig. 2.

In order to obtain an accurate result for dynamic performance, however, it is necessary to take into account a large number of the harmonics. An alternative and more realistic method is to use the actual back-EMF and current waveforms in state variable form. Using this method, the structure of the rotor of the BLDC motor and its high resistivity allows the neglect of induced currents in the rotor. This simplifies the modeling because there is no need to take into account the rotor damper windings effects and the related equations can be eliminated [13].

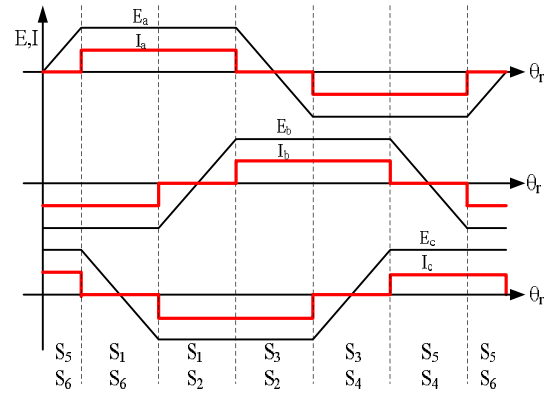


**Fig.2.** Back EMF pattern and reference current generation

### 3- Analysis of the Proposed Drive System

#### 3.1. Four-switch three-phase BLDC motor drive description

Fig. 3 shows the configuration of a four-switch inverter for a three-phase BLDC motor. According to Fig. 3, two common capacitors are used instead of a pair of bridges, and phase c is out of control because it is connected to the midpoint of the series capacitors. Compared with the conventional six-switch three-phase inverter for the BLDC motor, the whole working process of the BLDC motor in this paper is divided into six modes, as shown in Table 1.

**Table.1.** Working Mode of the Four-Switch Three-Phase BLDC Motor

Mode	Hall values	Working phase	Current Restraint	Conducting devices
1	101	+a, -b	$i_a = I^*, i_b = -I^*$	S <sub>1</sub> , S <sub>4</sub>
2	100	+a, -c	$i_a = I^*$	S <sub>1</sub>
3	110	+b, -c	$i_b = I^*$	S <sub>3</sub>
4	010	+b, -a	$i_b = I^*, i_a = -I^*$	S <sub>2</sub> , S <sub>3</sub>
5	011	+c, -a	$i_a = -I^*$	S <sub>2</sub>
6	011	+c, -b	$i_b = -I^*$	S <sub>4</sub>

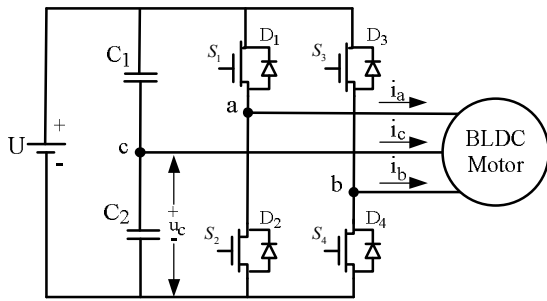


**Fig.3.** Four-switch three-phase inverter

Phase  $c$  involves four modes, including modes 2, 3, 5, and 6. Only one switch should work in the four modes. These modes are divided into two sub-operating modes. In modes 1 and 4, phases  $a$  and  $b$  have current flowing through them, and  $i_c$  should be equal to zero.

To avoid current waveform distortion, appropriate switch signals should be used in different working modes respectively, which imply that some new control schemes should be developed.

Here, mode 1 is taken as an example to demonstrate the whole working process that is identical in mode 4. Mode 1 is divided into four sub-operating modes, i.e. modes 11, 12, 13, and 14, as shown in Fig. 4. Switches  $S_1$  and  $S_4$  work in mode 11 with  $u_a = U$  and  $u_b = 0$ . Diodes  $D_2$  and  $D_3$  work in mode 12 with  $u_a = 0$  and  $u_b = U$ . Switch  $S_1$  and diode  $D_3$  work in mode 13 with  $u_a = U$  and  $u_b = U$ . Switch  $S_4$  and diode  $D_2$  work in mode 14 with  $u_a = 0$  and  $u_b = 0$ .

According to Fig. 4, the four sub-operating modes have different rules for adjusting the phase currents.

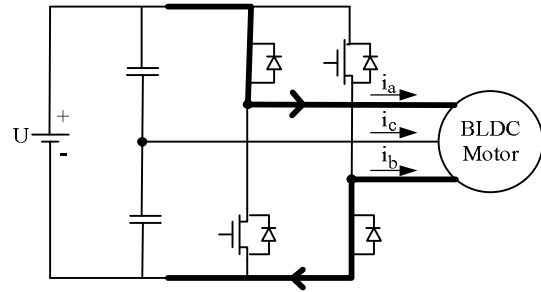


**Fig.4.a.** Sub-operating modes of model Mode 11

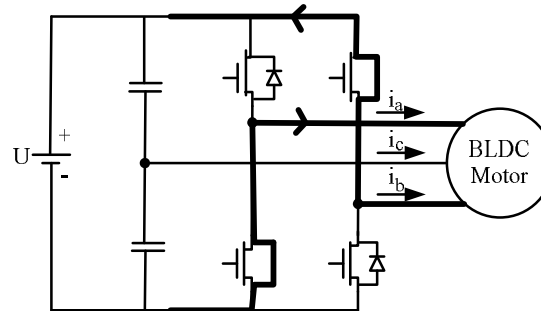


**Fig.4.b.** Sub-operating modes of model Mode 12

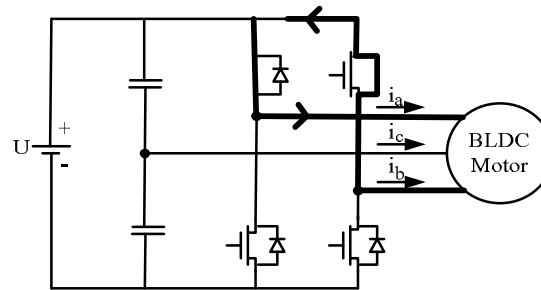


**Fig.4.c.** Sub-operating modes of model Mode 13

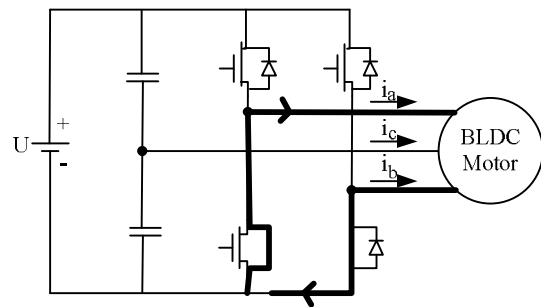


**Fig.4.d.** Sub-operating modes of model Mode 14

In mode 11,  $i_a$  and  $-i_b$  rise quickly, and  $i_c$  varies proportionally with the back EMF of phase  $c$ . In mode 12,  $i_a$  and  $-i_b$  drop quickly, and  $i_c$  changes proportionally with the back EMF of phase  $c$ . Compared with modes 11 and 12,  $i_c$  falls much quicker in mode 13 and rises much quicker in mode 14. In fact, when  $i_c$  deviates significantly from zero, modes 13 and 14 work properly. When  $i_c$  remains at zero, modes 11 and 12 work. Because  $i_a$  and  $i_b$  cannot be detected, a speed loop and Hall signals are used here to decide the duty of PWM signals.

### 3.2. Control of drive system using single current sensor

The whole control system is shown in Fig. 5. The control system adopts the double-loop structure. The inner current loop maintains the rectangular current waveforms, limits the maximum current, and ensures the stability of the system. The outer speed loop is designed to improve the static and dynamic characteristics of the system. The system performance is decided by the outer loop. If the disturbance caused by the inner loop, it can be limited by the outer loop. As shown in Fig. 5, the whole control system is made up of three controllers as follows:

*Controller 1:* Based on the position Hall signals, controller 1 works when the motor runs at modes 2, 3, 5, and 6. The schematic of controller 1 is shown in Fig. 6. As the PID controller has a simple structure, high efficiency, and easy implementation, the simple PID controller is used as a speed controller in this paper. The speed error can be represented as follows:

$$e(t) = \omega^* - \omega(t) \quad (5)$$

Where,  $\omega^*$  is the reference speed value and  $\omega(t)$  is the measured speed value at time  $t$ . The output of the speed PID controller is the threshold value of the current regulator  $I^*(t)$ . The simple hysteresis controller is also used as a current regulator. The input of the current regulator is:

$$e_i(t) = I^*(t) - i_c(t) \quad (6)$$

$u_1(t)$  is the duty of PWM signals.

*Controller 2:* In modes 1 and 4,  $I_{th}$  is close to zero. When  $|i_c| < I_{th}$ ,  $i_c$  is regarded as equal to zero, and consequently,  $i_a = -i_b$ . Controller 2 works at this stage, and phase a and b switch synchronously based on the speed loop, just as the traditional six-switch method does, as shown in Fig. 7.

The input of controller 2 is:

$$e(t) = \omega^* - \omega(k) \quad (7)$$

*Controller 3:* When the motor runs at modes 1 and 4, and  $I_{th} - |i_c| < 0$ , controller 3 works instead of controller 2, as shown in Fig. 8. When  $|i_c| > I_{th}$  and  $i_c > 0$ , based on the Hall signals, the strategy is at the stage of sub-operating mode 13 or mode 43 (switch  $S_3$  work in mode 43) and the magnitude of  $i_c$  drops quickly. If  $i_c = 0$ , the control flow will quit from controller 3. When  $|i_c| > I_{th}$  and  $i_c < 0$ , the strategy is at the stage of sub-operating mode 14 or mode 44 (switch  $S_2$  work in mode 44), and the magnitude of  $i_c$  rises quickly. If  $i_c = 0$ , the control flow will quit from controller 3.

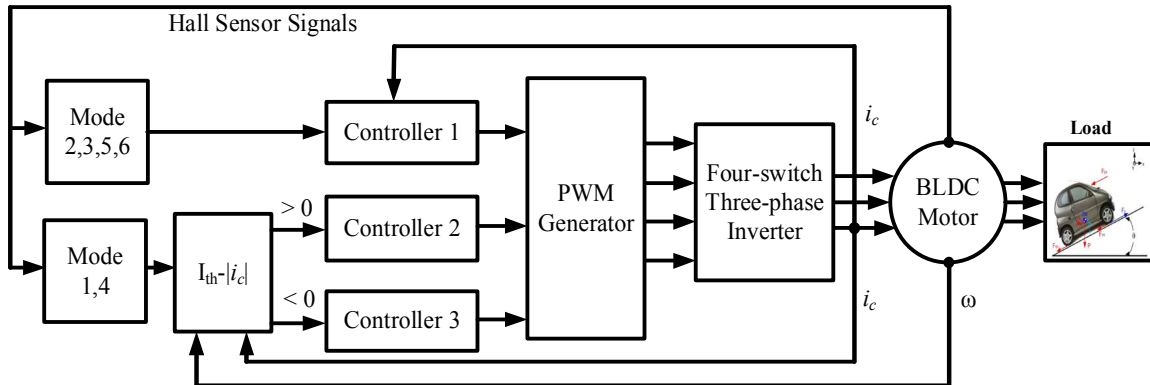


Fig.5. Schematic of the whole control system

Above all, the purpose of controller 3 is to keep Adjustment to working phase current should be done by controller 2, after controller 3 quits.

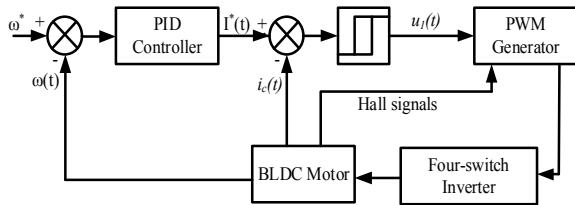


Fig.6. Schematic of controller 1

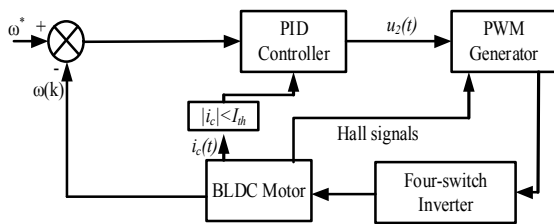


Fig.7. Schematic of controller 2

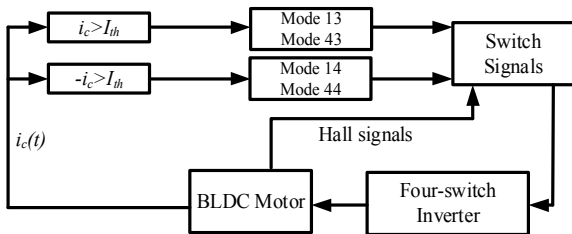


Fig.8. Schematic of controller 3

#### 4- Simulation Results

To evaluate the performance of the proposed drive system, simulation models have been established using MATLAB/Simulink. The main parameters of BLDC motor are as follows: inverter rated DC-link voltage 300 VDC, 1.5 kW, 1500 rpm, 2 poles,  $r_s = 0.4 \Omega$ ,  $L_s = 13 \text{ mH}$ , total rotor and load inertia  $J_T = 4 \times 10^{-3} \text{ kg.m}^2$ , torque constant  $0.4 \text{ V}/(\text{rad}/\text{sec})$ . The sampling interval is  $5 \mu\text{sec}$ , and magnitude of the current hysteresis band is  $0.2 \text{ A}$ .

A conventional PWM scheme for the six-switch inverter is used for the four-switch inverter topology of the BLDC motor drive, and its phase current waveforms are shown in Fig. 9. From Fig. 9, it is noted that  $i_c$  cannot be hold at zero, and it causes an additional and unexpected current, resulting in current distortion in phases  $a$  and  $b$ , and even in the breakdown of the system.

The same problem is inherited by the four-switch mode, and it causes the produced voltage vectors to be limited and asymmetric, which were well known as asymmetric voltage vectors. This problem has been solved by proposed control strategy in this paper.

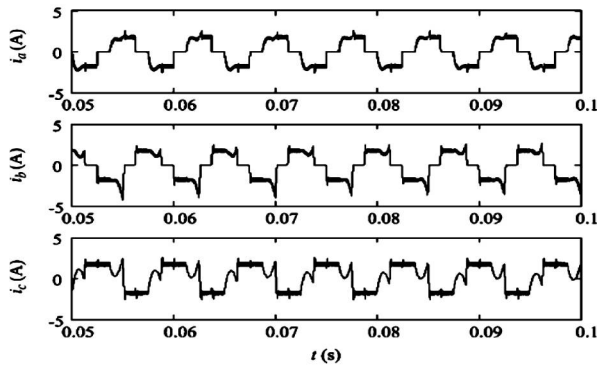


**Fig. 9.** Phase current waveforms of the four-switch three-phase BLDC motor when it is controlled by the conventional PWM strategy.

Speed, phase currents and electromagnetic torque waveforms of the proposed drive system are depicted in Fig. 10, when the four-switch three-phase BLDC motor is controlled by the single current sensor strategy.

The quasi-square waveforms of phase currents using proposed method verify the good control capability of BLDC motor in comparison to conventional methods. As shown in Fig. 10, the current and torque ripples in conduction region are eliminated effectively. The torque spikes in commutation region are also very low.

## 5- Conclusions

Improve the drive system reliability and optimizing software design are the key points to implement the proposed strategy in industrial application for further research. This paper introduced a new cost-effective BLDC

motor drive. Cost saving is achieved by reducing the number of inverter switches and current sensors. The single current sensor control strategy is used by the outer control loop to develop the performance of speed control that leads to the same characteristics of six-switch converter for the proposed four-switch inverter. In spite of conventional method, the proposed control strategy is able to control the motor in case of inverter switches' fault (up to two switches fault) using one current sensor and appropriate speed control loop. Finally, the proposed strategy has been verified successfully by simulation results.

## References

- [1] A. Darba, F. De Belie, P. D'haese and J. A. Melkebeek, "Improved Dynamic Behavior in BLDC Drives Using Model Predictive Speed and Current Control," in IEEE Transactions on Industrial Electronics, vol. 63, no. 2, pp. 728-740, Feb. 2016.
- [2] A. H. Niassar, A. Vahedi, and H. Moghbeli, "Analysis and control of commutation torque ripple in four-switch three-phase brushless DC motor drive," in Proc. IEEE Ind. Technol. Conf., 2006, pp. 239-246.
- [3] A. H. Niasar, H. Moghbeli, and A. Vahedi, "Adaptive neuron-fuzzy control with fuzzy supervisory learning algorithm for speed regulation of 4-switch inverter brushless DC machines," in Proc. IEEE Power Electron. Motion Control Conf., 2006, pp. 1-5.
- [4] A. H. Niasar, A. Vahedi, and H. Moghbeli, "A novel position sensorless control of a four-switch, brushless DC motor drive without phase shifter," IEEE Trans. Power Electron., vol. 23, no. 6, pp. 3079-3087, Nov. 2008.
- [5] A. Rubaai and P. Young, "Hardware/Software Implementation of Fuzzy-Neural-Network Self-Learning Control Methods for Brushless DC Motor Drives," in IEEE Transactions on

- Industry Applications, vol. 52, no. 1, pp. 414-424, Jan.-Feb. 2016.
- [6] B. K. Lee, T.H. Kim, M. Ehsani; "On the feasibility of four-switch three-phase BLDC motor drives for low cost commercial applications: topology and control", in IEEE Trans. Power Electron., vol. 18, no. 1, pp. 164-172, Jan 2003.
- [7] C. S. Joice, S. R. Paranjothi and V. J. S. Kumar, "Digital Control Strategy for Four Quadrant Operation of Three Phase BLDC Motor With Load Variations," in IEEE Transactions on Industrial Informatics, vol. 9, no. 2, pp. 974-982, May 2013.
- [8] D.-H. Jung and I.-J. Ha, "Low-cost sensorless control of brushless DC motors using a frequency-independent phase shifter," IEEE Trans. Power Electron., vol. 15, no. 4, pp. 744-752, Jul. 2000.
- [9] J.-H. Lee, T.-S. Kim, and D.-S. Hyun, "A study for improved of speed response characteristic in four-switch three-phase BLDC motor," in Proc. IEEE Ind. Electron. Soc. Conf., 2004, vol. 2, pp. 1339-1343.
- [10] J.-H. Lee, S.-C. Ahn, and D.-S. Hyun, "A BLDCM drive with trapezoidal back EMF using four-switch three phase inverter," in Conf. Rec. IEEE IAS Annu. Meeting, 2000, vol. 3, pp. 1705-1709.
- [11] J. Shao, D. Nolan, M. Teissier, and D. Swanson, "A novel microcontroller-based sensorless brushless dc (BLDC) motor drive for automotive fuel pumps," IEEE Trans. Ind. Appl., vol. 39, no. 6, pp. 1730-1740, Nov./Dec. 2003.
- [12] M. Ebadpour, M R. AlizadehPahlavani, "Performance Analysis and the Cost Effective Position Sensorless Control of Axial Flux PM Brushless DC Motor," Journal of Asian Electric Vehicles, vol. 11, no. 2, pp. 1645-1651 December 2013.
- [13] P.Pillay and R.Krishnan, "Modeling, Simulation and Analysis of Permanent Magnet Motor Drives, Part II: The Brushless DC Motor Drive," IEEE Transactions on Industrial Applications, vol.25, no.2, pp.274-279, Apr 1989.

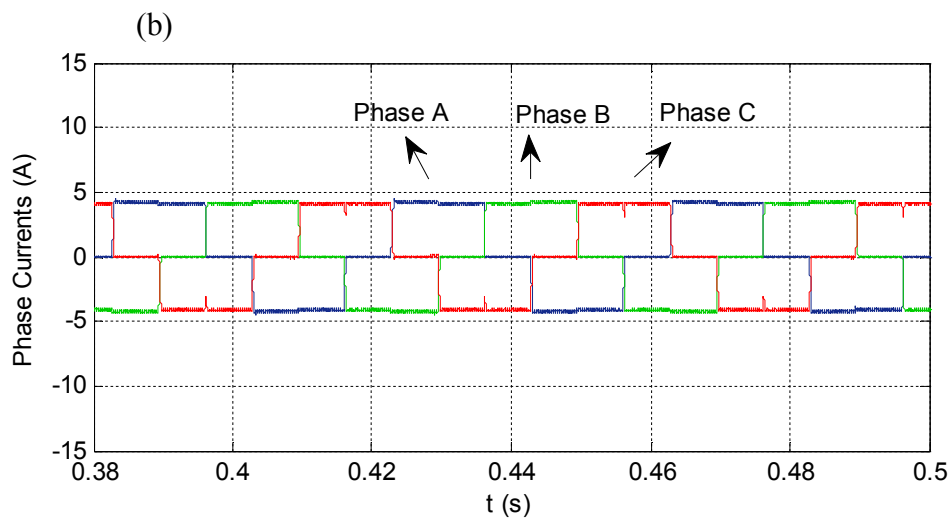
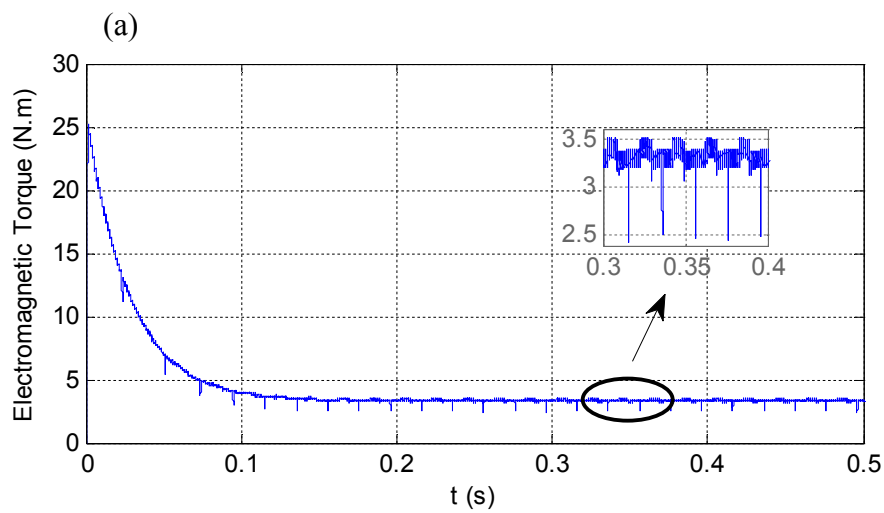
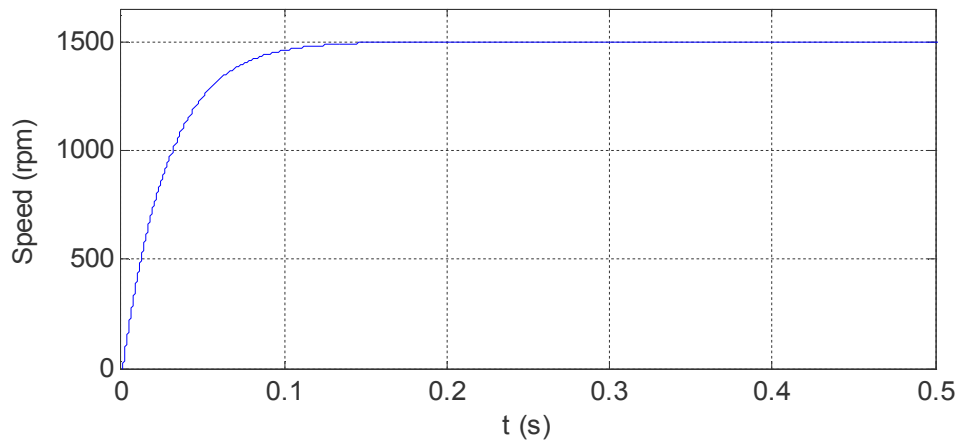


**Fig. 10.** Simulation waveforms when the motor is controlled by the single current sensor strategy; (a) Speed curve, (b) Electromagnetic torque curve, (c) Phase current waveforms